



Supplement of

Estimates of mass absorption cross sections of black carbon for filter-based absorption photometers in the Arctic

Sho Ohata et al.

Correspondence to: Sho Ohata (sho.ohata@isee.nagoya-u.ac.jp)

The copyright of individual parts of the supplement might differ from the article licence.

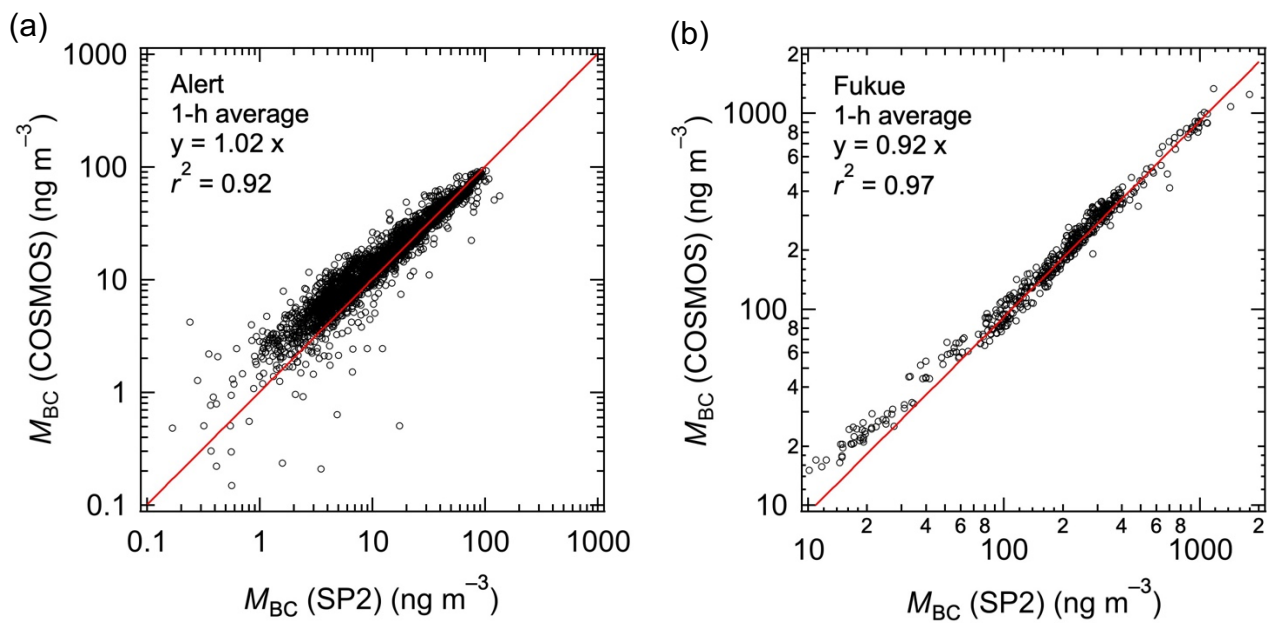
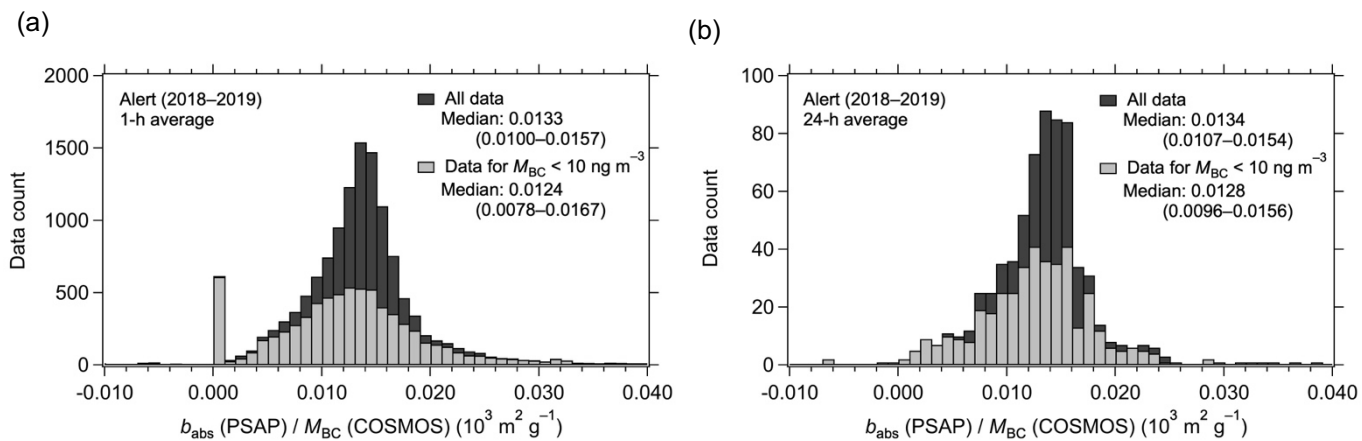
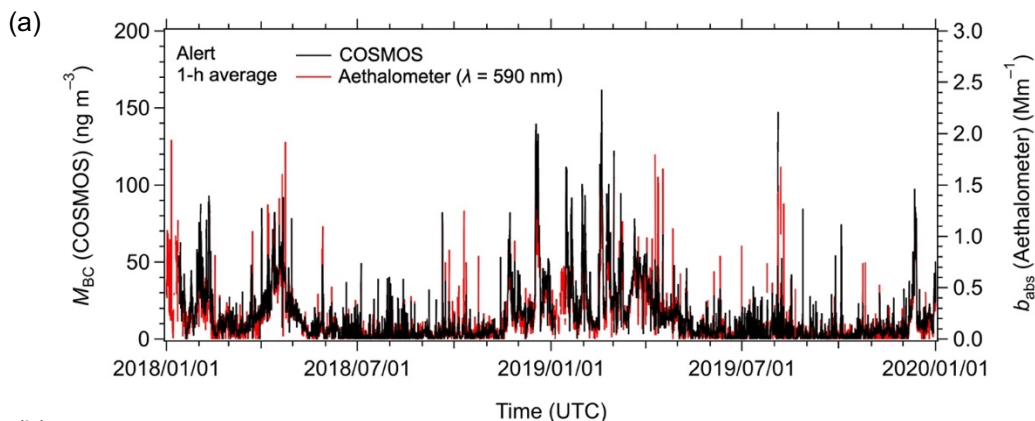


Figure S1. Correlation of M_{BC} measured by COSMOS and SP2 at (a) Alert and (b) Fukue. The axes are on a logarithmic scale. The solid line in the correlation plot is the least squares regression forced through the origin.

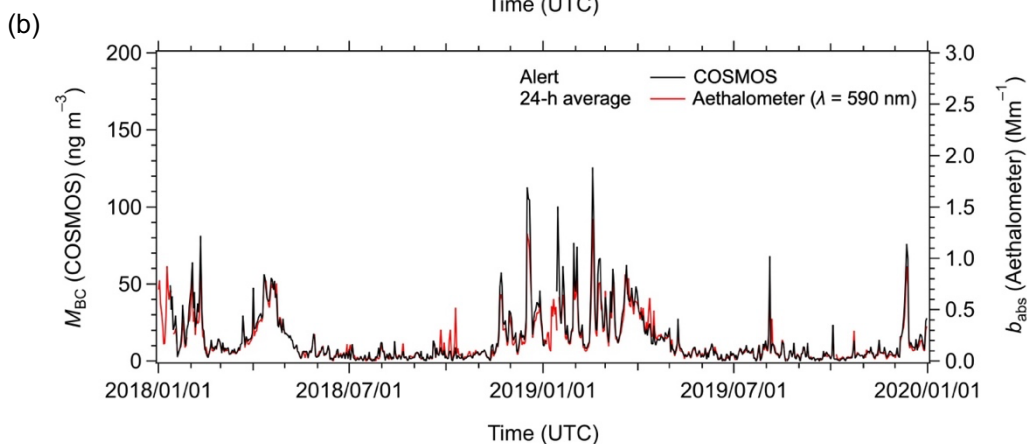


10 **Figure S2.** Histograms of $b_{\text{abs}}(\text{PSAP}; \lambda = 550 \text{ nm}) / M_{\text{BC}}(\text{COSMOS})$ ratios at Alert for (a) 1-h averaged and (b) 24-h averaged data. Histograms for all data and data with $M_{\text{BC}}(\text{COSMOS}) < 10 \text{ ng m}^{-3}$ are shown. The interquartile ranges are shown in parentheses.

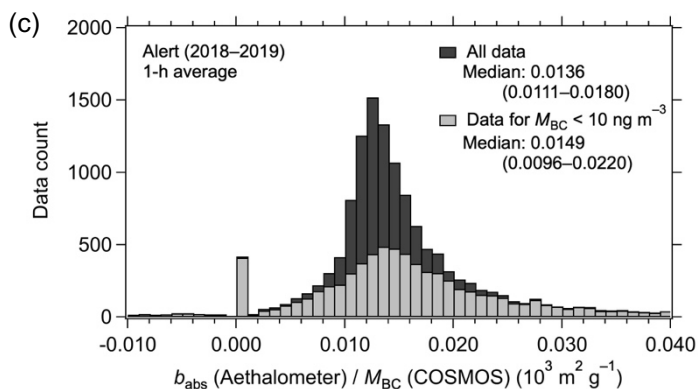
15



20



25



30

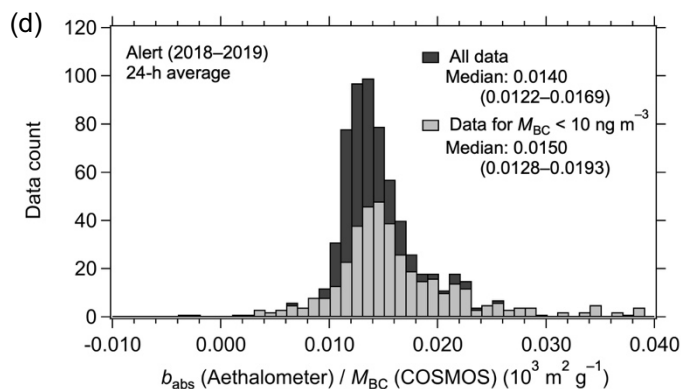
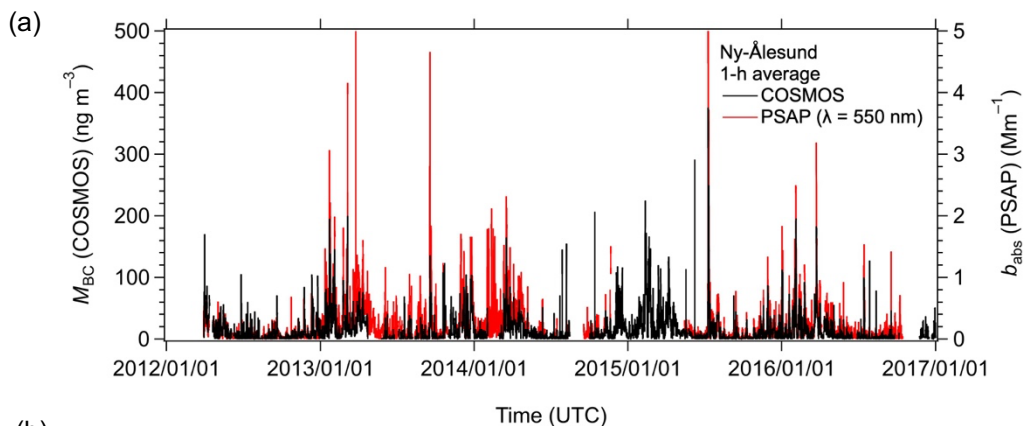
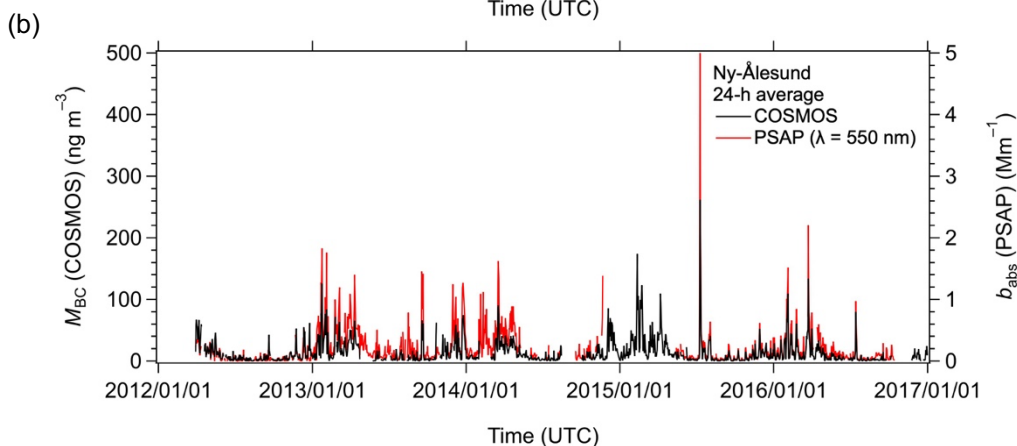


Figure S3. Time series of M_{BC} (COSMOS) and b_{abs} (Aethalometer; $\lambda = 590$ nm) from January 2018 to December 2019 at Alert for (a) 1-h averaged and (b) 24-h averaged data. (c) and (d) Corresponding histograms of b_{abs} (Aethalometer) / M_{BC} (COSMOS) ratios for all data and data with M_{BC} (COSMOS) < 10 ng m^{-3} . The interquartile ranges are shown in parentheses.

35

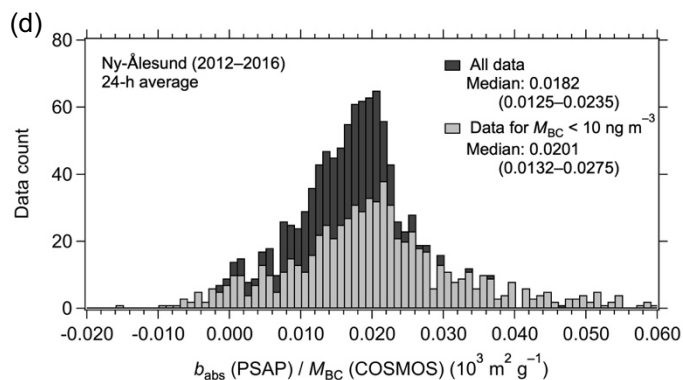
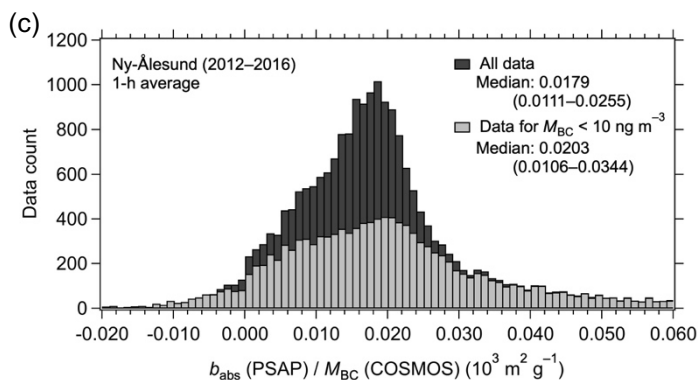


40



45

50



55

Figure S4. Time series of M_{BC} (COSMOS) and b_{abs} (PSAP; $\lambda = 550 \text{ nm}$) from April 2012 to September 2016 at Ny-Ålesund for (a) 1-h averaged and (b) 24-h averaged data. (c) and (d) Corresponding histograms of b_{abs} (PSAP) / M_{BC} (COSMOS) ratios for all data and data with M_{BC} (COSMOS) $< 10 \text{ ng m}^{-3}$. The interquartile ranges are shown in parentheses.

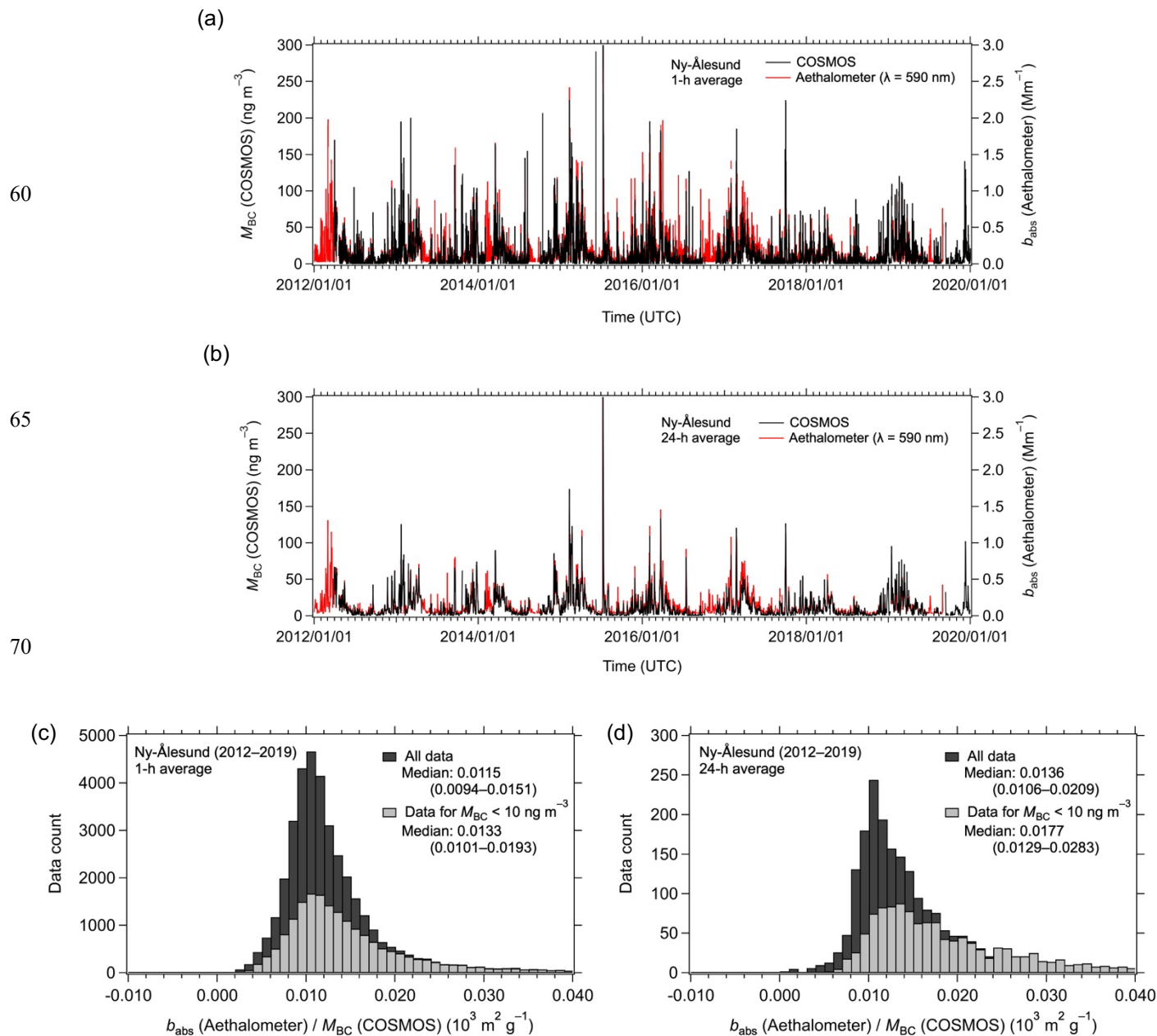


Figure S5. Time series of M_{BC} (COSMOS) and b_{abs} (Aethalometer; $\lambda = 590$ nm) from April 2012 to August 2019 at Ny-Ålesund for (a) 1-h averaged and (b) 24-h averaged data. (c) and (d) Corresponding histograms of b_{abs} (Aethalometer) / M_{BC} (COSMOS) ratios for all data and data with M_{BC} (COSMOS) < 10 ng m^{-3} . The interquartile ranges are shown in parentheses.

75

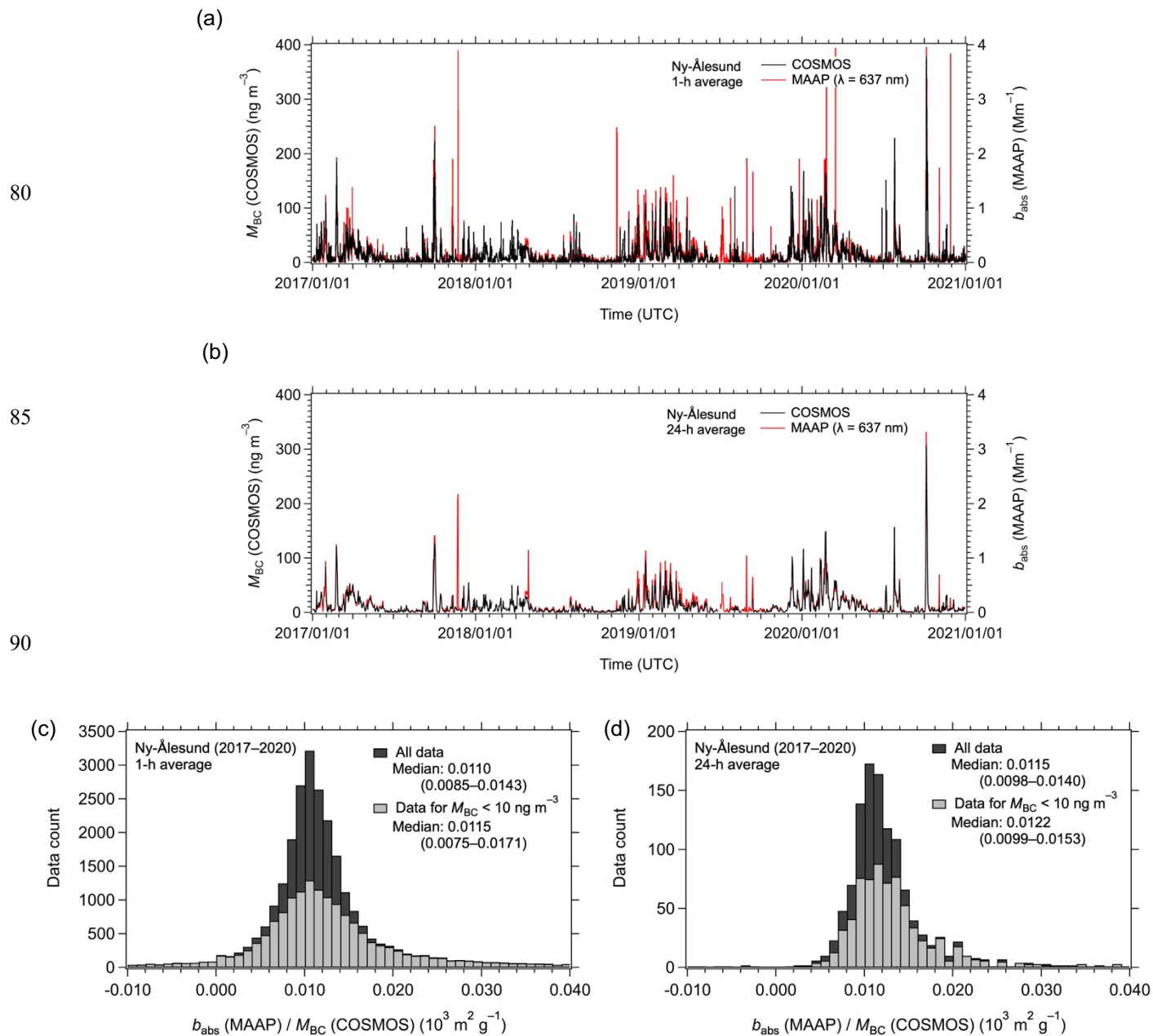


Figure S6. Time series of M_{BC} (COSMOS) and b_{abs} (MAAP; $\lambda = 637$ nm) from January 2017 to December 2020 at Ny-Ålesund for (a) 1-h averaged and (b) 24-h averaged data. (c) and (d) Corresponding histograms of b_{abs} (MAAP) / M_{BC} (COSMOS) ratios for all data and data with M_{BC} (COSMOS) $< 10 \text{ ng m}^{-3}$. The interquartile ranges are shown in parentheses.

95

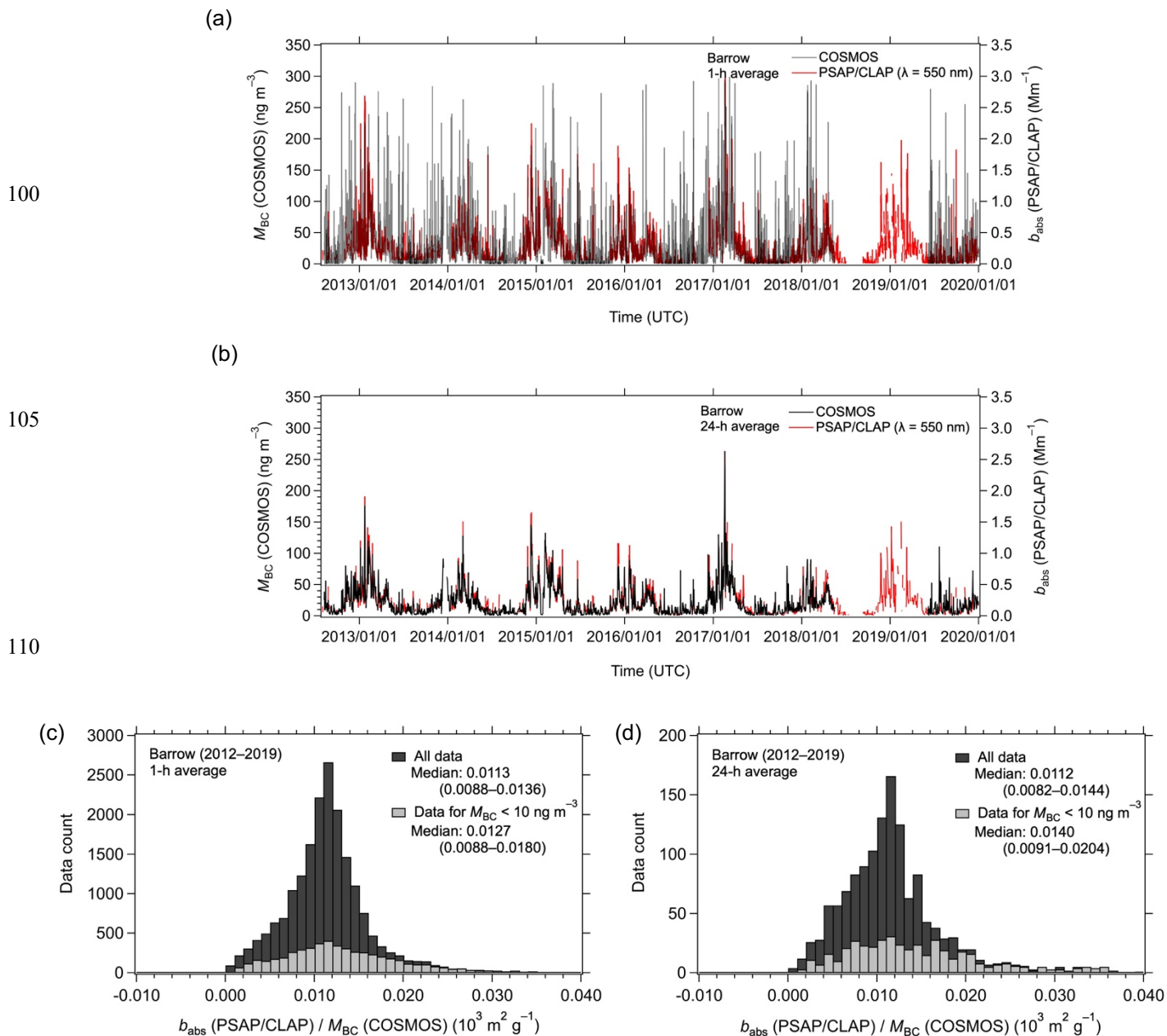


Figure S7. Time series of M_{BC} (COSMOS) and b_{abs} (PSAP/CLAP; $\lambda = 550 \text{ nm}$) from August 2012 to December 2019 at Barrow for (a) 1-h averaged and (b) 24-h averaged data. (c) and (d) Corresponding histograms of b_{abs} (PSAP/CLAP) / M_{BC} (COSMOS) ratios for all data and data with M_{BC} (COSMOS) < 10 ng m^{-3} . The interquartile ranges are shown in parentheses.

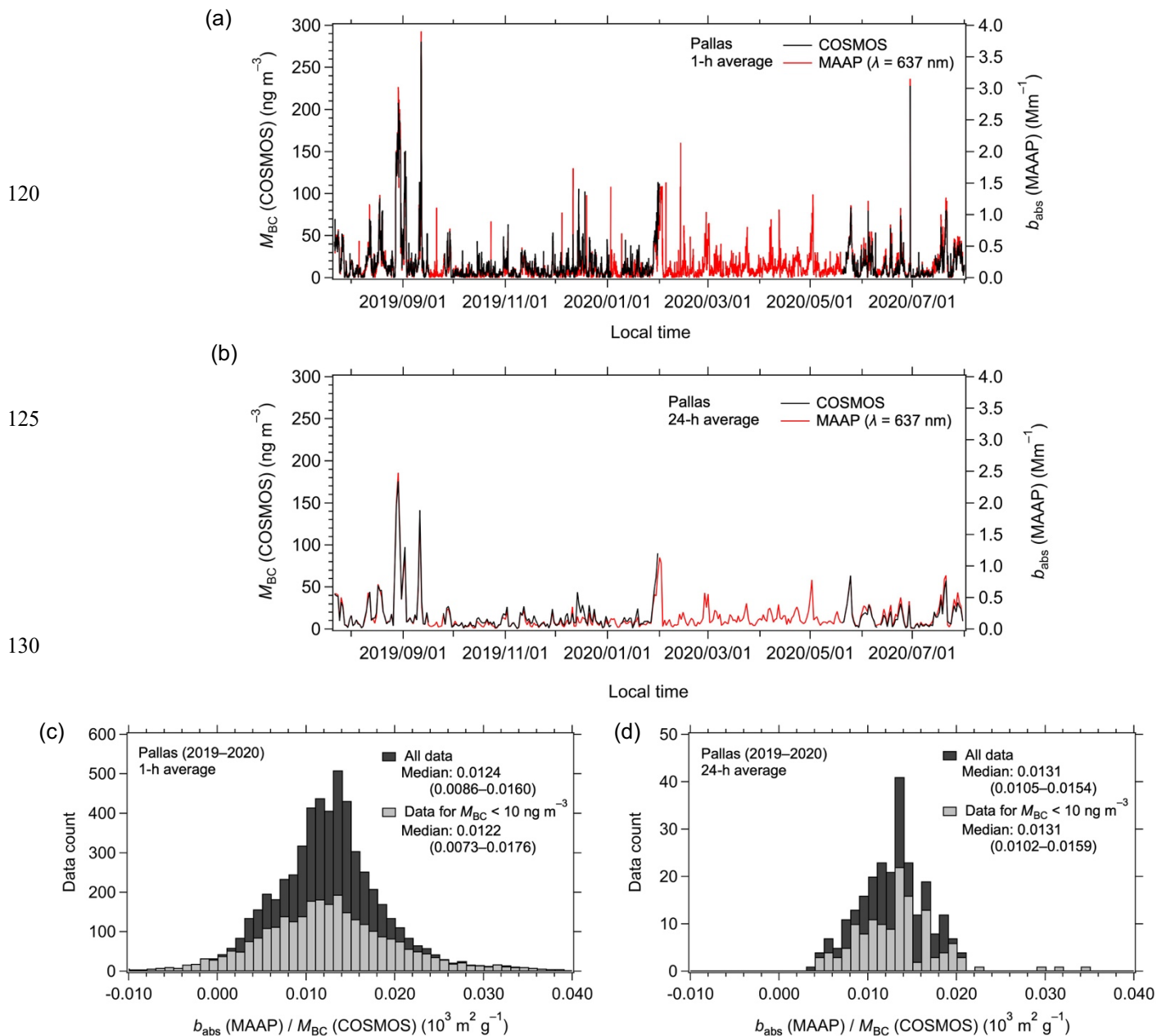


Figure S8. Time series of M_{BC} (COSMOS) and b_{abs} (MAAP; $\lambda = 637 \text{ nm}$) from July 2019 to July 2020 at Pallas for (a) 1-h averaged and (b) 24-h averaged data. (c) and (d) Corresponding histograms of b_{abs} (MAAP) / M_{BC} (COSMOS) ratios for all data and data with M_{BC} (COSMOS) $< 10 \text{ ng m}^{-3}$. The interquartile ranges are shown in parentheses.

135

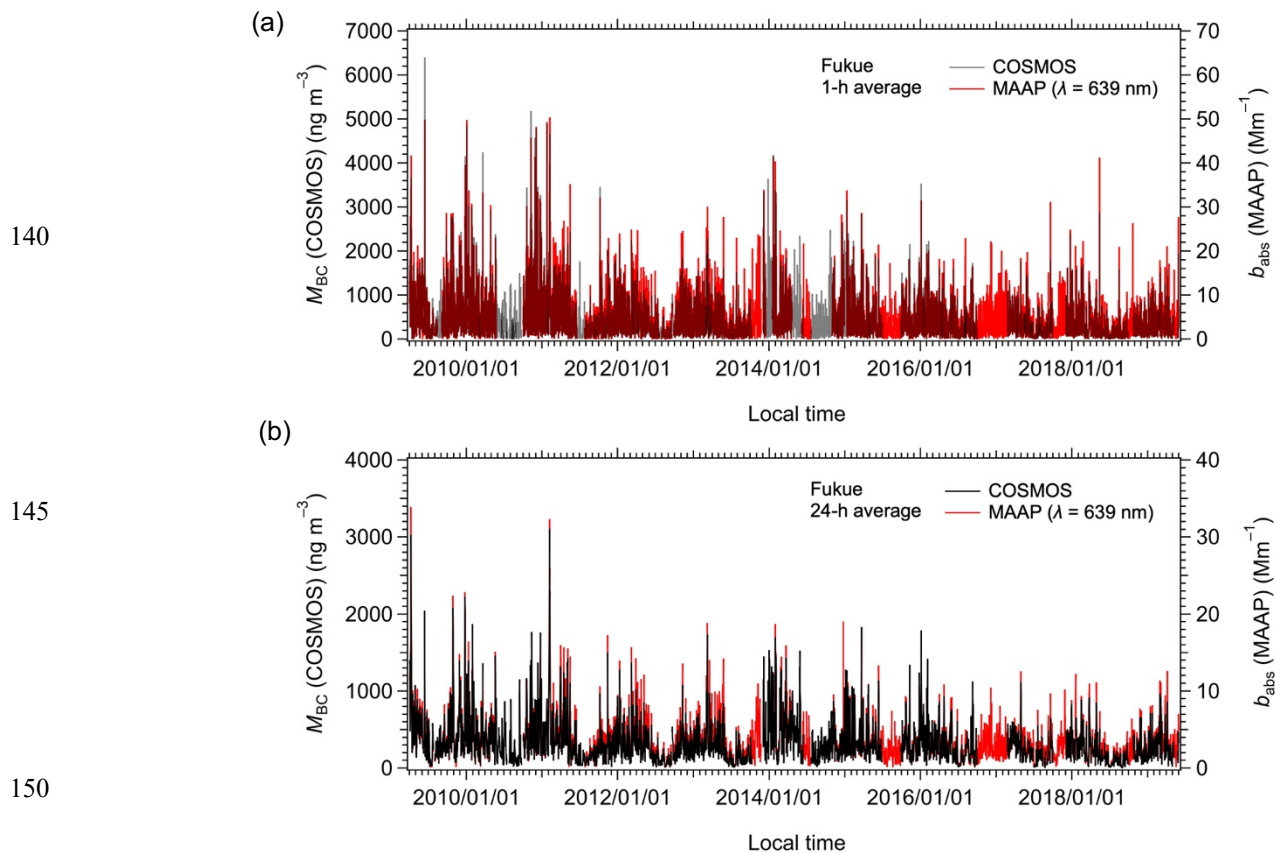


Figure S9. Time series of M_{BC} (COSMOS) and b_{abs} (MAAP; $\lambda = 590$ nm) from April 2009 to May 2019 at Fukue for (a) 1-h averaged and (b) 24-h averaged data.

155